# Heterostructure-Barrier-Varactor Design

Jan Stake, *Member, IEEE*, Stephen H. Jones, *Member, IEEE*, Lars Dillner, Stein Hollung, *Member, IEEE*, and Erik L. Kollberg, *Fellow, IEEE*

*Abstract*—In this paper, we propose a simple set of accurate frequency-domain design equations for calculation of optimum embedding impedances, optimum input power, bandwidth, and conversion efficiency of heterostructure-barrier-varactor (HBV) frequency triplers. A set of modeling equations for harmonic balance simulations of HBV multipliers are also given. A 141-GHz quasi-optical HBV tripler was designed using the method and experimental results show good agreement with the predicted results.

*Index Terms*—HBV, varactor frequency tripler.

## I. INTRODUCTION

**T**HE heterostructure-barrier-varactor (HBV) diode is ideally suited for frequency tripling in the millimeter- and submillimeter-wave regime. The symmetric capacitance-voltage characteristic of the HBV allows for tripler design without requiring a second-harmonic idler circuit or dc bias. In principle, this should make HBV triplers easier to design than Schottky diode triplers. However, the complex device structure and device physics makes the overall tripler design process more difficult. In particular, the design and fabrication of the semiconductor device is more difficult than Schottky diode structures used in similar applications.

When first introduced by Kollberg *et al.*, the HBV design focused on mesa structures for whisker contacting and calculation of the small-signal dc characteristics [1]. This work was followed by a more complete and detailed harmonic-balance-analysis-based design [2] and the fabrication of 2.5%–4.8% efficient planar geometry HBV's operating at 230–260 GHz [3]–[5]. Most recently, excellent HBV tripler results demonstrating an efficiency of 12% at 247 GHz with a 28 $\mu$m$^2$ area device have been reported by Mélique *et al.* [6]. These results clearly indicate that HBV's offer the best overall solution for millimeter-wave frequency triplers.

In order to continue the general utilization of HBV's, we offer a complete set of design equations for millimeter-wave HBV's. The equations are based upon the well-known analysis of Penfield and Rafuse [7] and can easily be used to calculate the optimum input power, optimum embedding impedances, bandwidth, and efficiency of HBV triplers. For convenience, the entire analysis given below can be easily run from the Internet via a Java interface by visiting devicesim.ee.virginia.edu.

TABLE I
HBV GENERIC LAYER STRUCTURE

| Layer No. | | Thickness [Å] | Doping level [cm$^{-3}$] |
|---|---|---|---|
| 7 | Contact | ~ 3000 | $n^{++}$ |
| 6 | Modulation | $l$ ~ 3000 | $N_d$ ~ $10^{17}$ |
| 5 | Spacer | $s$ ~ 50 | Undoped |
| 4 | Barrier | $b$ ~ 200 | Undoped |
| 3 | Spacer | $s$ ~ 50 | Undoped |
| 2 | Modulation | $l$ ~ 3000 | $N_d$ ~ $10^{17}$ |
| 1 | Buffer | | $n^{++}$ |
| 0 | Substrate | | $n^{++}$ or SI |

## II. HBV MULTIPLIER FREQUENCY-DOMAIN DESIGN EQUATIONS

### A. Analysis Overview

The analysis given below is an extension of the Schottky diode analysis in reference [8], and similar to the analysis of varactor diodes presented by Penfield and Rafuse [7], Burckhardt [9], Tang [10], as well as Krishnamurthi *et al.* [11]. Expressions describing the device nonlinear charge, nonlinear resistance, maximum applied voltage at breakdown, and parasitic resistance are combined with a frequency-domain impedance analysis in order to derive simple design expressions for optimum HBV triplers. The resulting design equations for embedding impedances, efficiency, input power, and bandwidth are for maximum conversion efficiency only. Using these equations and by varying the diode parameters, the effect on optimum multiplier performance can be explored. The proposed set of quick-design equations should be used as a starting point in an HBV tripler design procedure. The multiplier performance as a function of embedding impedances and further adjustments of the circuit must be explored with a more detailed large-signal simulator.

### B. Analysis of Device Parameters

A generic layer structure of an HBV is shown in Table I. For multiple epitaxially stacked barriers, the layer sequence 2–5 is repeated $N$ times. The intrinsic part of the HBV consists of layers 2–6, where a high bandgap material (layer 4) prevents electron transport through the structure and the diode capacitance is modulated due to the depletion of carriers in layers 2 and 6.

In our analysis, we use a two-element model of the HBV multiplier: a nonlinear (differential) elastance $S(v_j) = dv_j/dQ = 1/C(v_j)$ in series with a nonlinear parasitic resistance $R(v_j)$. Since varactor mode of operation for HBV's is preferred, the diode is not allowed to be driven harder than the turn-on voltage $v_{j,\max}$ for large conduction current ($dV/dI \gg S_{\max}/\omega_p$).

During a pump cycle, the elastance is modulated due to the depletion of carriers and the overall elastance can, therefore, be expressed as the sum of a constant term and a nonlinear part as

$$S(t) = \frac{\partial v_j(t)}{\partial Q}$$
$$= \frac{N}{A}\left(\frac{b}{\varepsilon_b} + \frac{2s}{\varepsilon_d}\right) + \underbrace{S_a(t)}_{\text{accumulation}} + \underbrace{S_d(t)}_{\text{depletion}} \quad 1/\text{F} \qquad (1)$$

where $b$ and $s$ are given in Table I, and

$\varepsilon_b$      dielectric constant of the barrier material;
$\varepsilon_d$      dielectric constant of the modulation region;
$v_j$      voltage across the capacitor;
$Q$      charge stored in the HBV;
$A$      device area;
$S_a(t)$      elastance due to accumulation of carriers;
$S_d(t)$      elastance due to depletion of carriers.

The minimum elastance $S_{\min}$ of an HBV is determined by the effective distance between charges on each side of the barrier. For a typical HBV structure (see Table I), the minimum elastance can be estimated as

$$S_{\min} = \min\left(S(t)\right) = \frac{N}{A}\left(\frac{b}{\varepsilon_b} + \frac{2s}{\varepsilon_d} + \frac{2L_D}{\varepsilon_d}\right) \quad 1/\text{F} \tag{2}$$

where $L_D$ is the extrinsic Debye length

$$L_D = \sqrt{\frac{kT\varepsilon_d}{q^2 N_D}}. \tag{3}$$

If a smaller bandgap material is used for the spacer layers, the charges on each side of the barrier are confined in quantum wells adjacent to the barrier, which reduces the conduction current and increases the $C_{\max}/C_{\min}$ ratio [12], [13]. In this case, the second term in (2) reduces to $\sim s/\varepsilon_d$ and the $L_D$ term should be dropped.

The maximum elastance $S_{\max}$ during a pump cycle is determined by the drive level of the HBV, defined as

$$\text{drive} \equiv \frac{\max\left(Q(t)\right)}{Q_{\max}} \tag{4}$$

where $Q_{\max}$ is the charge at the turn-on voltage $v_{j,\max}$. Thus, drive $\leq 1$ is equivalent to varactor mode of operation and drive $>1$ corresponds to operation between varistor and varactor mode. Optimum performance is achieved with maximum elastance swing and negligible conduction current compared to the displacement current and drive $= 1$. Thus, the maximal extension of the depletion region $w_{\max}$ is determined by the maximum electric field at breakdown $E_{\max}$ or the effect of current saturation [14], [15]. Hence, the maximum elastance swing is determined by one of the following conditions:

Condition 1: depletion layer punch-through $w_{\max} = l$;
Condition 2: large electron conduction across the barrier region at high electric fields;
Condition 3: large electron conduction from impact ionization at high electric fields;

Condition 4: saturated electron velocity in the material determines the maximum length an electron can travel during a quarter of a pump cycle.

Referring to condition 2, the conduction current is a strong function of the barrier height discontinuity and the electric field in the barrier. How to solve for $E_{\max}$ under condition 2 is given in [16]. For condition 3, $E_{\max}$ is a function of the doping concentration and can be calculated as described in [17]. Knowing $E_{\max}$, $w_{\max}$ can be calculated as

$$w_{\max} = \frac{\varepsilon_d E_{d,\max}}{q N_d}. \tag{5}$$

The average electron velocity during one-half of the pump cycle for an HBV is $v_{\text{avg}} = 4w_{\max}f_p$. This value cannot exceed the saturated electron velocity for the material $v_{\max}$. For condition 4, the maximum length $w_{\max}$ can be estimated as

$$w_{\max} = \frac{v_{\text{avg}}}{4f_p} = \frac{v_{\max}}{4kf_p}. \tag{6}$$

To compensate for the current waveform, inertial, and other high-frequency effects, an additional factor $k$ is used. For Schottky diodes, the maximum extension is determined by $w_{\max} = v_{\max}/(2kf_p)$ [18]. Louhi *et al.* [15] have proposed $k = n$ for Schottky diode design, where $n$ is the order of multiplication. Assuming a sinusoidal current waveform, one can easily show that $k$ is equal to $\pi/2$. From harmonic-balance analysis of HBV triplers, we have found that $k$ is typically between 1.5–2 and, hence, we suggest $k = 2$.

Thus, for nominal operation drive $= 1$, the maximal elastance is limited by

$$S_{\max} = \max\left(S(t)\right) = \frac{N}{A}\left(\frac{b}{\varepsilon_b} + \frac{2s}{\varepsilon_d} + \frac{w_{\max}}{\varepsilon_d}\right) \tag{7}$$

and the corresponding maximal voltage across the capacitor can be estimated as

$$v_{j,\max} = N\varepsilon_d E_{d,\max}\left(\frac{b}{\varepsilon_b} + \frac{2s}{\varepsilon_d} + \frac{E_{d,\max}}{2qN_d}\right). \tag{8}$$

The parasitic series resistance is the sum of the resistance of the undepleted active layers, the spreading resistance [19], and the ohmic contact resistance. The resistance of the undepleted layers contributes to the intrinsic varactor model. All extrinsic impedances can be regarded as a part of the embedding circuit. If the modulation layers, i.e., 2 and 6 in Table I, are homogeneously doped and an abrupt space charge is assumed, the series resistance can be expressed as a function of the length of the depleted region $w(t)$ as

$$R(t) = \underbrace{R_p + \frac{\rho_d l}{A}(1+N)}_{=R_s} - \frac{\rho_d w(t)}{A}N = R_s - \frac{\rho_d w(t)}{A}N \tag{9}$$

where

$R_p$      extrinsic series resistance (contact resistance, spreading resistance, etc.);
$R_s$      zero-bias series resistance;

$w$  length of the depleted region;
$l$  thickness of the epitaxial modulation layer (2 and 6 in Table I);
$\rho_d$  resistivity of the modulation layer

$$\rho_d = \frac{1}{qN_D\mu_e(N_D, T)}. \tag{10}$$

Since the resistance (9) is varying with respect to the variation in the elastance, the above equation can be rewritten as

$$R(t) = R_s - \rho_d\varepsilon_d\underbrace{\left(S_d(t) + S_f(t)\right)}_{=S'_d(t)} = R_s - \rho_d\varepsilon_d S'_d(t). \tag{11}$$

At high frequencies, the maximum elastance is reduced (6), (7) and the edge of the depleted region is smeared out and its sharpness varies with time [20]. Therefore, the elastance $S_d(t)$ is modified by $S_f(t)$ at high frequencies in our model.

### C. Frequency-Domain Analysis of HBV Impedance

The voltage across the symmetric HBV is

$$v(t) = R(t)i(t) + v_j(t)$$
$$= R_s i(t) - \rho_d\varepsilon_d S'_d(t)i(t) + \int S(t)i(t)\,dt. \tag{12}$$

The voltage waveform, current waveform, and elastance waveforms can be represented in the frequency domain as a Fourier series, and the circuit equation takes the following form for the $k$th harmonic [7], [8]:

$$V_k = R_s I_k + \frac{S_{\min}}{jk\omega_p}I_k + \frac{\sum_{l=-\infty}^{\infty}I_l S_{d, k-l}}{jk\omega_p}$$
$$-\rho_d\varepsilon_d\sum_{l=-\infty}^{\infty}I_l S'_{d, k-l}. \tag{13}$$

Furthermore, by defining the complex modulation ratio as $M_k = S_k/(S_{\max} - S_{\min})$, the general form of the large-signal device impedance $Z_{d, k}$ can be written as

$$Z_{d, k} = R_s + \frac{S_{\min}}{jk\omega_p} + (S_{\max} - S_{\min})$$
$$\cdot \left(\frac{1}{jk\omega_p}\frac{1}{I_k}\sum_{l=-\infty}^{\infty}I_l M_{d, k-l}\right.$$
$$\left. - \rho_d\varepsilon_d\frac{1}{I_k}\sum_{l=-\infty}^{\infty}I_l M'_{d, k-l}\right). \tag{14}$$

The summation over all current and elastance harmonics in (14) yields a complex number that depends on the embedding circuit conditions and on the physical properties of the HBV itself. To determine the maximum conversion efficiency, i.e., when the pump power is completely absorbed and power delivered to the load at the third harmonic is maximized, we assume that the complex summation is independent of external conditions and the HBV layer structures. Consequently, the optimal embedding

TABLE II
HBV DESIGN COEFFICIENTS

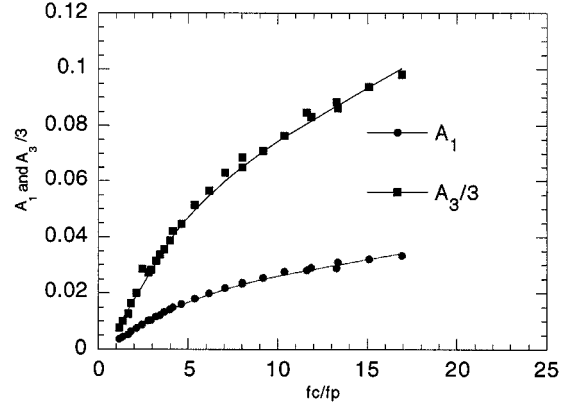| Extraction conditions: $f_p/f_c < 0.2$ | | |
|---|---|---|
| $B_1 = 0.3$ | $C_1 = 0.2$ | $D_1 = -2.7$ |
| $B_3 = 0.5$ | $C_3 = -0.1$ | $D_3 = -1.1$ |
| $\alpha = 200$ | $\beta = 1.5$ | $\gamma = 0.8$ |



Fig. 1.  Design coefficients $A_1$ and $A_3/3$ versus $f_c/f_p$.

impedances $Z_{c, n}$ for the HBV multiplier close to any operating condition can be expressed as

$$R_{c, 1} \approx R_s + (S_{\max} - S_{\min})\left(\frac{A_1}{\omega_p} - \rho_d\varepsilon_d C_1\right)$$
$$X_{c, 1} \approx \frac{S_{\min}}{\omega_p} + (S_{\max} - S_{\min})\left(\frac{B_1}{\omega_p} - \rho_d\varepsilon_d D_1\right)$$
$$R_{c, 3} \approx R_s + (S_{\max} - S_{\min})\left(\frac{A_3}{3\omega_p} - \rho_d\varepsilon_d C_3\right)$$
$$X_{c, 3} \approx \frac{S_{\min}}{3\omega_p} + (S_{\max} - S_{\min})\left(\frac{B_3}{3\omega_p} - \rho_d\varepsilon_d D_3\right) \tag{15}$$

where $A_n$, $B_n$, $C_n$, and $D_n$ are fitting coefficients. These coefficients can be determined by optimizing the circuit for maximum efficiency using harmonic-balance analysis. We have determined the coefficients for a wide range of device and circuit parameters (see Table II and Fig. 1). Hence, (15) can be used as a starting point to design the embedding circuit and a fairly ideal impedance match of the diode at the first and third harmonic frequencies will be achieved.

By introducing the dynamic cutoff frequency $\omega_c = (S_{\max} - S_{\min})/R_s$ of a varactor [7], the above expressions for optimal impedances can be rewritten as

$$\frac{Z_{c, 1}}{R_s} = 1 + \frac{S_{\min}}{R_s\omega_p}j + \frac{f_c}{f_p}\left(A_1 + jB_1 - \rho_d\varepsilon_d\omega_p(C_1 + jD_1)\right)$$
$$\frac{Z_{c, 3}}{R_s} = 1 + \frac{S_{\min}}{3R_s\omega_p}j + \frac{f_c}{f_p}\left(\frac{A_3 + jB_3}{3} - \rho_d\varepsilon_d\omega_p(C_3 + jD_3)\right) \tag{16}$$

where the dynamic cutoff frequency of a typical HBV can be derived from (2), (7), and (9) as

$$f_c = \frac{1}{2\pi}\frac{N(w_{\max} - 2L_D)}{\varepsilon_d\left(AR_p + \rho_d l(1 + N)\right)}. \tag{17}$$
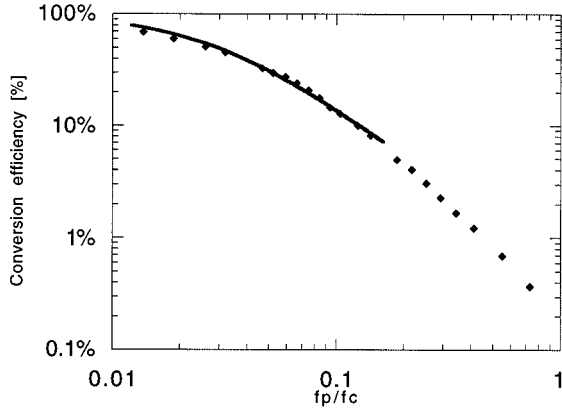
Fig. 2. Optimum conversion efficiency of HBV triplers simulated using the model (21) and (22) described in Section III. The solid line is a curve fit using (18) ($\alpha = 200$, and $\beta = 1.5$).

Equation (16) is similar to the result of Penfield and Rafuse [7] for Schottky diodes, but with additional terms $C_n$ and $D_n$ accounting for the high-frequency and large-signal nonlinear resistance of the device. It is also similar to the result obtained in [8] for Schottky diodes. However, the values of the coefficients shown in Table II are different, and an additional capacitance term is introduced. To maximize $f_c$, the parasitic resistance $R_p$ should be minimized and $w_{\max}$ should be large compared to $L_d$.

### D. Pump Power and Conversion Efficiency

The conversion efficiency $\eta$ is defined as the power delivered to the load at the third harmonic divided by the available input power. For a varactor multiplier, the efficiency is related to the ratio of the pump frequency and the dynamic cutoff frequency [7], [21]. The maximum conversion efficiency can be estimated from the following empirical expression:

$$\eta \approx \frac{100}{1 + \alpha \left( \frac{f_p}{f_c} \right)^\beta} \, \% \tag{18}$$

where $\alpha$ and $\beta$ are extracted from detailed large-signal simulations for a wide range of devices and circuit conditions (see Table II and Fig. 2). To maximize the efficiency, the dynamic cutoff frequency $f_c$ in (17) should be maximized and $w_{\max} = l$ to avoid excessive losses. This maximum conversion efficiency is predicted for the optimal embedding impedances described by (16).

Finally, the necessary input power to modulate the elastance of an HBV from $S_{\min}$ to $S_{\max}$ can be estimated as

$$P_{\mathrm{AVA}} = \frac{R_{c,1}}{2|Z_{d,1}|^2} |V_1|^2 \approx \gamma \frac{R_{c,1}}{2|Z_{c,1} - R_s|^2} |v_{j,\max}|^2 \tag{19}$$

where $\gamma$ is a fitting coefficient (see Table II). Equation (19) ensures that reasonable device parameters and required input powers are designed for a particular application.

### E. Bandwidth Analysis

The maximum bandwidth $B$, at which power can be coupled to the HBV input circuit, can be estimated from the Bode–Fano criteria for linear networks [22]. Under this condition, $B$ is given by

$$B = \frac{\pi f_p R_{c,1}}{-X_{c,1} \log(\Gamma)} \tag{20}$$

where $\Gamma$ is the reflection coefficient at the HBV input, $f_p$ is the pump frequency, and $X_{c,1}$ and $R_{c,1}$ are calculated using the coefficients in Table II and (16). As expected, very high-efficiency HBV multipliers can only be impedance matched over a narrow frequency band.

### III. HBV Models for Harmonic-Balance Simulation

The theory above [i.e., (16)–(20)] is intended as a quick-design method and as a starting point for a more detailed harmonic-balance-design investigation. The device model described in this section is used to extract the coefficients in the previous section over a broad range of operating conditions. It can be used to model the performance of a complete multiplier circuit [23]. The voltage across the HBV capacitance and its displacement current can be expressed as [24]

$$v_j(Q) = N \left( \frac{bQ}{\varepsilon_b A} + 2 \frac{sQ}{\varepsilon_d A} + \mathrm{Sign}(Q) \right.$$
$$\left. \cdot \left( \frac{Q^2}{2qN_d\varepsilon_d A^2} + \frac{4kT}{q} \left( 1 - e^{-|Q|/2L_D A q N_d} \right) \right) \right)$$
$$i(t) = \frac{\partial Q}{\partial t}. \tag{21}$$

The model is accurate for drive $<1$ and can easily be implemented in any harmonic-balance simulator. Furthermore, given the above voltage–charge relation, the parasitic series resistance can be expressed as

$$R(Q) = R_s - \frac{\rho_d N}{A} \left( \frac{|Q|}{qN_d A} + 2L_D \left( e^{-|Q|/2L_D A q N_d} - 1 \right) \right). \tag{22}$$

This model can be extended to include the conduction current [4] (drive $> 1$). For a more detailed physical quasi-statical description, see Adamski et al. [25]. For detailed HBV analysis, codes combining time-dependent drift–diffusion numerical device analysis with frequency-domain harmonic-balance analysis can be used [2], [26]; this simulation code can also be run from the internet via a Java interface using devicesim.ee.virginia.edu.

### IV. Results and Discussion

#### A. Parameter Extraction for Optimal Design

All the coefficients were extracted by analyzing the HBV structure shown in Table III with the model described in Section III implemented in HP-MDS. The conversion efficiency was maximized by tuning the embedding impedances at the first and third harmonic, respectively. For the coefficient extraction, pump frequencies of 100 and 50 GHz were used. All simulations were performed by assuming a homogeneous temperature of $T = 300$ K across the active device region, a device area of 50 $\mu m^2$, and a field-independent (low field) electron mobility of $\mu_e = 4375$ cm$^2$/V·s in the GaAs region. Simulations were performed over a wide range of operating conditions,

TABLE III
NU2003 LAYER STRUCTURE

| Material | Doping [cm$^{-3}$] | Thickness [Å] |
|---|---|---|
| InAs | 1×10$^{19}$ | 100 |
| In$_{1-x}$GaAs | 1×10$^{19}$ | 400 |
| GaAs | 1×10$^{19}$ | 3000 |
| GaAs | 8×10$^{16}$ | 2500 |
| GaAs | Undoped | 35 |
| Al$_{0.7}$GaAs | Undoped | 200 |
| GaAs | Undoped | 35 |
| GaAs | 8×10$^{16}$ | 5000 |
| GaAs | Undoped | 35 |
| Al$_{0.7}$GaAs | Undoped | 200 |
| GaAs | Undoped | 35 |
| GaAs | 8×10$^{16}$ | 2500 |
| GaAs | 1×10$^{19}$ | 40000 |
| GaAs | SI | - |

$0.01 < f_p/f_c < 1$, by changing the drive level and the series resistance $R_s$. Finally, coefficients for the design equations (16), (18), and (19) were extracted (see Table II and Fig. 1). The maximum tripler conversion efficiency versus $f_p/f_c$ (Fig. 2) is obtained by using (18) and the coefficients $\alpha$ and $\beta$ given in Table II. Coefficients $B_n$, $C_n$, and $D_n$ were found to be independent of the $f_c/f_p$ ratio, as expected. However, $A_1$ and $A_3$ are related to the conversion efficiency and, hence, functions of $f_p/f_c$, as shown in Fig. 1. These coefficients allow the optimum embedding impedances and the efficiency to be easily calculated for a wide range of device parameters.

### B. Design Example

A 3 × 47 GHz quasi-optical tripler was designed and fabricated using the quick-design method above [27]. The planar four-barrier HBV diodes (UVA-NRL-1174-17) used for this circuit have a device area of 57 $\mu$m$^2$ and a material structure, as shown in Table III. The quick-design procedure is as follows.

1) A parasitic resistance $R_p = 12\ \Omega$ was estimated for the HBV [4]. With an electron mobility of $\mu_e = 4375$ cm$^2$/Vs, the total series resistance $R_s$ can be calculated to 16 $\Omega$.
2) The maximum extension of the depletion region $w_{\max}$ is given by one of the four conditions described in Section II-B; the smallest value for $w_{\max}$ becomes the limiting case. For this particular device, high conduction current due to self-heating determines the maximum elastance swing (case 2). Assuming a device temperature of 350 K, $w_{\max}$ was calculated to 2000 Å, as described in [16].
3) A cutoff frequency of 1 THz is estimated from (17).
4) The optimum embedding impedances can be calculated using (16), Table II, and Fig. 1: $Z_{c,1} = 28 + 241\ j\Omega$ and $Z_{c,3} = 52 + 103\ j\Omega$ (single device).
5) A maximum HBV tripler efficiency of 33% is estimated from (18).
6) Finally, the required pump power is estimated to 26 mW from (19).

Two diodes were soldered in parallel to lower the required circuit impedances and increase the power-handling capability.

The circuit was further optimized using harmonic-balance analysis with an HBV model [4] including conduction current through the structure. The optimum embedding impedances were adjusted to $Z_{c,1} = 16 + 126\ j\Omega$ and $Z_{c,3} = 22 + 53\ j\Omega$ for two diodes in parallel and a pump power of 25 mW. These impedance values are very close to the values quickly designed above in 4). Furthermore, the measured overall peak efficiency of the HBV tripler circuit was 9% for an input power of 31 mW per diode [27]. Input loss and output loss were estimated to 1 and 3.5 dB, respectively, for this circuit. The diode efficiency is calculated to 25% for an absorbed input power of 25 mW per diode. Experimental results verify that efficiency, optimal embedding impedances, and required pump power agree well with the above quick-design results [27].

## V. CONCLUSIONS AND SUMMARY

We have described a complete model for prediction of optimum embedding impedances, pump power, and efficiency of HBV triplers. The models can be used over a broad range of frequencies for a variety of HBV devices and circuits. Comparisons with experimental results are favorable. Based on the analysis described here, a new set of HBV's have been designed and will be tested in the near future. The HBV quick-design method is available on-line through the web-interface http://devicesim.ee.virginia.edu.
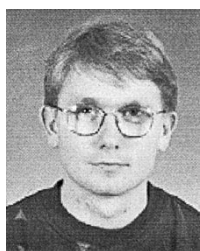
## REFERENCES

[1] E. L. Kollberg and A. Rydberg, "Quantum-barrier-varactor diode for high efficiency millimeter-wave multipliers," *Electron. Lett.*, vol. 25, pp. 1696–1697, 1989.
[2] J. R. Jones, G. B. Tait, S. H. Jones, and S. D. Katzer, "DC and large-signal time-dependent electron transport in heterostructure devices: An investigation of the heterostructure barrier varactor," *IEEE Trans. Electron Devices*, vol. 42, pp. 1393–1403, Aug. 1995.
[3] J. R. Jones, W. L. Bishop, S. H. Jones, and G. B. Tait, "Planar multibarrier 80/240 GHz heterostructure barrier varactor triplers," *IEEE Trans. Microwave Theory Tech.*, vol. 45, pp. 512–518, Apr. 1997.
[4] J. Stake, L. Dillner, S. H. Jones, C. M. Mann, J. Thornton, J. R. Jones, W. L. Bishop, and E. L. Kollberg, "Effects of self-heating on planar heterostructure barrier varactor diodes," *IEEE Trans. Electron Devices*, vol. 45, pp. 2298–2303, Nov. 1998.
[5] J. Stake, C. M. Mann, L. Dillner, S. H. Jones, S. Hollung, M. Ingvarson, H. Mohamed, B. Alderman, and E. L. Kollberg, "Improved diode geometry for planar heterostructure barrier varactors," presented at the 10th Int. Space Terahertz Technol. Symp., Charlottesville, VA, 1999.
[6] X. Mélique, A. Maestrini, E. Lheurette, P. Mounaix, M. Favreau, O. Vanbésien, J. M. Goutoule, G. Beaudin, T. Nähri, and D. Lippens, "12% Efficiency and 9.5 dBm output power from InP-based heterostructure barrier varactor triplers at 250 GHz," presented at the IEEE-MTT Int. Microwave Symp., Anaheim, CA, 1999.
[7] P. Penfield and R. P. Rafuse, *Varactor Applications*. Cambridge, MA: MIT Press, 1962.
[8] R. E. Lipsey and S. H. Jones, "Accurate design equations for 50–600 GHz GaAs Schottky diode varactor frequency doublers," *IEEE Trans. Electron Devices*, vol. 45, pp. 1876–1882, Sept. 1998.
[9] C. B. Burckhardt, "Analysis of varactor frequency multipliers for arbitrary capacitance variation and drive level," *Bell Syst. Tech. J.*, pp. 675–692, 1965.

[10] C. C. H. Tang, "An exact analysis of varactor frequency multiplier," *IEEE Trans. Microwave Theory Tech.*, vol. MTT-14, pp. 210–212, Apr. 1966.

[11] K. Krishnamurthi and R. G. Harrison, "Analysis of symmetric-varactor frequency triplers," in *IEEE-MTT Int. Microwave Symp. Dig.*, vol. 2, 1993, pp. 649–652.

[12] J. R. Jones, S. H. Jones, and G. B. Tait, "GaAs/InGaAs/AlGaAs heterostructure barrier varactors for frequency tripling," presented at the 5th Int. Symp. Space Terahertz Technol., Ann Arbor, MI, 1994.

[13] V. Duez, X. Mélique, O. Vanbésien, P. Mounaix, F. Mollot, and D. Lippens, "High capacitance ratio with GaAs/InGaAs/AlAs heterostructure quantum well-barrier varactors," *Electron. Lett.*, vol. 34, pp. 1860–1861, 1998.

[14] E. L. Kollberg, T. J. Tolmunen, M. A. Frerking, and J. R. East, "Current saturation in submillimeter wave varactors," *IEEE Trans. Microwave Theory Tech.*, vol. 40, pp. 831–838, May 1992.

[15] J. T. Louhi and A. V. Räisänen, "On the modeling and optimization of Schottky varactor frequency multipliers at submillimeter wavelengths," *IEEE Trans. Microwave Theory Tech.*, vol. 43, pp. 922–926, Apr. 1995.

[16] J. Stake, L. Dillner, S. H. Jones, E. L. Kollberg, and C. M. Mann, "Design of 100-900 GHz AlGaAs/GaAs planar heterostructure barrier varactor frequency triplers," presented at the 9th Int. Space Terahertz Technol. Symp., Pasadena, CA, 1998.

[17] S. M. Sze, *Physics of Semiconductor Devices*. New York: Wiley, 1981, p. 103.

[18] T. W. Crowe, T. C. Grein, R. Zimmermann, and P. Zimmermann, "Progress toward solid-state local oscillators at 1 THz," *IEEE Microwave Guided Wave Lett.*, vol. 6, pp. 207–208, May 1996.

[19] L. E. Dickens, "Spreading resistance as a function of frequency," *IEEE Trans. Microwave Theory Tech.*, vol. MTT-15, pp. 101–109, Feb. 1967.

[20] R. E. Lipsey, S. H. Jones, J. R. Jones, L. F. Horvath, U. V. Bhapkar, T. W. Crowe, and R. J. Mattauch, "Monte Carlo harmonic-balance and drift-diffusion harmonic-balance analyses of 100–600 GHz Schottky barrier varactor frequency multipliers," *IEEE Trans. Electron Devices*, vol. 44, pp. 1843–1849, Nov. 1997.

[21] L. Dillner, J. Stake, and E. L. Kollberg, "Analysis of symmetric varactor frequency multipliers," *Microwave Opt. Technol. Lett.*, vol. 15, pp. 26–29, 1997.

[22] R. M. Fano, "Theoretical limitations on the broadband matching of arbitrary impedances," *J. Franklin Inst.*, vol. 249, 1950.

[23] L. Dillner, M. Oldfield, and C. M. Mann, "The complete analytical simulation of heterostructure barrier varactor frequency multipliers," presented at the 10th Int. Space Terahertz Technol. Symp., Charlottesville, VA, 1999.

[24] L. Dillner, J. Stake, and E. L. Kollberg, "Modeling of the heterostructure barrier varactor diode," presented at the Int. Semiconductor Device Res. Symp., Charlottesville, VA, 1997.

[25] M. E. Adamski, M. T. Faber, and J. A. Dobrowolski, "Heterostructure barrier varactor multiplier simulation using physics based quasistatic charge model," presented at the 28th European Microwave Conf., Amsterdam, Holland, 1998.

[26] M. F. Zybura, J. R. Jones, S. H. Jones, and G. B. Tait, "Simulation of 100-300-GHz solid-state harmonic sources," *IEEE Trans. Microwave Theory Tech.*, vol. 43, pp. 955–961, Apr. 1995.

[27] S. Hollung, J. Stake, L. Dillner, and E. L. Kollberg, "A 141-GHz quasioptical HBV diode frequency tripler," presented at the 10th Int. Space Terahertz Technol. Symp., Charlottesville, VA, 1999.

**Jan Stake** (M'95) was born in Uddevalla, Sweden, in 1971. He received the Civilingenjör (M.Sc.) degree in electrical engineering, and the Tekn.Lic. and Ph.D. degrees in microwave electronics from Chalmers University of Technology, Göteborg, Sweden, in 1994, 1996, and 1999, respectively.

While a Ph.D. student, he spent four months during 1997 at the University of Virginia, Charlottesville. He is currently a Research Scientist at the Rutherford Appleton Laboratory (RAL), Didcot, U.K. His interests are devices for millimeter-wave applications and device fabrication technologies.

**Stephen H. Jones** (S'85–M'89) received the B.Sc., M.Sc., and Ph.D. degrees in electrical and computer engineering from the University of Massachusetts at Amherst, in 1984, 1987, and 1989, respectively.

After being with at Millitech Corporation briefly, he joined the faculty in the Electrical Engineering Department, University of Virginia, Charlottesville. He has co-authored over 70 technical papers and holds two U.S. patents related to microelectronics science and technology. He is currently the President of Virginia Semiconductor Inc. (VSI), Fredericksburg, VA. VSI has been manufacturing 3- and 4-in as well as custom Si substrates for over 20 years for electronic device and sensor manufacturers around the world.

Dr. Jones has served as chairman of the International Semiconductor Device Research Symposium, chairman of the National Capital Section of the Electrochemical Society, and chairman of the Central Virginia Chapters of the IEEE Electron Devices and Microwave Theory and Techniques Societies. In 1993, he was awarded a Lilly Foundation National Teaching Fellowship, and in 1996, he was awarded the Lucien Carr III Professorship in Engineering.



**Lars Dillner** was born in Säffle, Sweden, in 1968. He received the M.S. degree in engineering physics and the Tekn.Lic. degree in microwave electronics from Chalmers University of Technology, Göteborg, Sweden, in 1994 and 1998, respectively, and is currently working toward the Ph.D. degree in microwave electronics at Chalmers University.

His research interests are varactor diodes and frequency multipliers.



**Stein Hollung** (S'96–M'98) was born in Oslo, Norway, on March 7, 1970. He received the electrical engineering degree from the Oslo College of Engineering, Oslo, Norway, in 1992, and the Ph.D. degree in electrical engineering from the University of Colorado at Boulder, in 1998.

He is currently a Research Scientist at Chalmers University of Technology, Göteborg, Sweden. His research interests include microwave and millimeter-wave circuits and antennas.



**Erik L. Kollberg** (M'83–SM'83–F'91) received the Teknologie Doktor degree from the Chalmers University of Technology, Göteborg, Sweden, in 1970.

In 1980, he became a Professor in the School of Electrical and Computer Engineering, and was the Acting Dean of electrical and computer engineering from 1987 to 1990. A major responsibility of his from 1967 to 1987 had been development of radio astronomy receivers working from a few gigahertz up to 250 GHz for the Onsala Space Observatory telescopes in both Sweden and Chile. From 1963 to 1976, his research was performed on low-noise maser amplifiers used for radio astronomy observations at the Onsala Space Observatory. Various types of masers were developed for the frequency range from 1 to 35 GHz. Eight such masers are or have been used for radio astronomy observations at the Onsala Space Observatory. In 1972, his research was initiated on low-noise millimeter-wave Schottky diode mixers, and in 1981, also on superconducting quasi-particle (SIS) mixers. This research covers device properties as well as mixer development for frequencies from about 30 to 750 GHz. In 1980, his research was initiated on GaAs millimeter-wave Schottky diodes, and since 1986, resonant tunneling devices and three terminal devices such as field-effect transistors (FET's) and heterojunction bipolar transistors (HBT's). He pointed out the limitation in performance of varactor multipliers due to current saturation effects. He is the inventor of the heterostructure barrier varactor diode. He performed early research on superconducting hot-electron mixers, and his group has achieved world-record results. In the fields mentioned above, he has published approximately 250 scientific papers. He was an Invited Guest Professor to Ecole Normal Superieure, Paris, France, during the summers of 1983, 1984, and 1987. From September 1990 to March 1991, he was an Invited Distinguished Fairchild Scholar at the California Institute of Technology.

Dr. Kollberg is a member of the Royal Swedish Academy of Science and the Royal Swedish Academy of Engineering Sciences. He received the 1982 Microwave Prize presented at the 12th European Microwave Conference, Helsinki, Finland, and the 1986 Gustaf Dahlén Gold Medal.